Medical Engineering and Physics 74 (2019) 121–128

Contents lists available at ScienceDirect

Medical Engineering and Physics

journal homepage: www.elsevier.com/locate/medengphy

The neochord mitral valve repair procedure: Numerical simulation of different neochords tensioning protocols

Luigi Di Micco[a,*], Paolo Peruzzo[a], Andrea Colli[b], Gaetano Burriesci[c,d], Daniela Boso[a], Laura Besola[e], Gino Gerosa[e], Francesca M. Susin[a]

[a] Cardiovascular Fluid Dynamics Laboratory, ICEA Department, University of Padova, Via Loredan 20, 35131 Padova, Italy
[b] Cardiac Thoracic and Vascular Department University of Pisa, Pisa, Italy
[c] UCL Mechanical Engineering, University College London, United Kingdom
[d] Ri.MED Foundation, Palermo, Italy
[e] DSCTV, University of Padova Medical School, Italy

ARTICLE INFO

Article history:
Received 9 July 2018
Revised 1 August 2019
Accepted 16 September 2019

Keywords:
NeoChord procedure
Mitral valve repair
Finite elements analysis
Tensioning strategies
Mitral valve prolapse

ABSTRACT

Transapical off-pump mitral valve repair with neochord implantation is an established technique for minimally-invasive intervention on mitral valve prolapse/flail. The procedure involves the positioning of artificial chords, whose length/tension is adjusted intraoperatively, adopting different methods based on the experience of the surgeon. This unsystematic approach occasionally leads to complications such as leaflet rupture and excessive/insufficient load on the neochords. In this study, finite element models of a generalized prolapsing mitral valve are used to verify the effect of two alternative tensioning approaches (AT – All together and 1-by-1 – one by one sequences) on the coaptation area and valve biomechanics, comparing results with a corresponding healthy configuration. The total force of about 1 N is exerted by the chords in both strategies, but the maximum stress and coaptation area are closer to those of the healthy configuration in the 1-by-1 sequence. However, the analysis also provides an explanation for the chords unloading in the 1-by-1 strategy observed in the clinical practice, and suggests an optimum tensioning methodology for NeoChord procedures. The study also reveals the potential power of the implemented numerical approach to serve as a tool for procedural planning, supporting the identification of the most suitable ventricular access site and the most effective stitching points for the artificial chords.

1. Introduction

Experimental and numerical investigations are nowadays largely used to assess the safety and efficacy of cardiovascular devices and procedures, by identifying an enhanced medical practice and support clinical decisions [1–6]. However, the application of these approaches to treatments of mitral valve (MV) diseases still represents a major challenge, due to the complex anatomy of the valvular and subvalvular apparatus.

Mitral regurgitation (MR) is one of the most complex valvular diseases. MR is classified into two categories: functional MR (FMR), due to left ventricular (LV) dilation and dysfunction, and degenerative MR (DMR), due to a structural abnormality of the valve apparatus, mainly. The latter can lead, among possible valve failures, to prolapse or flail [7–9]. Recently a new MV procedure with off-pump transcatheter access with neochord implantation has emerged as a new promising surgical procedure to restore the functionality of DMR [10,11]. It consists in the replacement of native chordae tendineae with artificial tethers, inserted by transapical access. The clinical outcome has confirmed the safety and effectiveness of the approach [12], enlightening the issues to be addressed to enhance the reliability of the procedure and support preoperative planning. In particular, the optimum tensioning of the artificial chords still needs to be determined, in order to maximize the efficacy of the technique and the durability of the solution [13]. This issue is further complicated by the fact that the transapical implantation approach results in non-physiological orientations of the artificial sutures, which load the leaflet along directions different from the native chordae

A number of in vitro and in silico studies have attempted to study the biomechanics of MV repair with neochords implantation [14–19] analyzing the post-implant configuration after the complete surgical procedure. Differently by the cited studies, the NeoChord procedure is performed in beating-heart. Consequently, in order to identify the most suitable implantation protocol end the commonly reported procedural complications, such as leaflet rupture or neochords overloading/unloading, the study of NeoChord

* Corresponding author.
E-mail address: luigi.dimicco@dicea.unipd.it (L. Di Micco).

https://doi.org/10.1016/j.medengphy.2019.09.014
1350-4533/

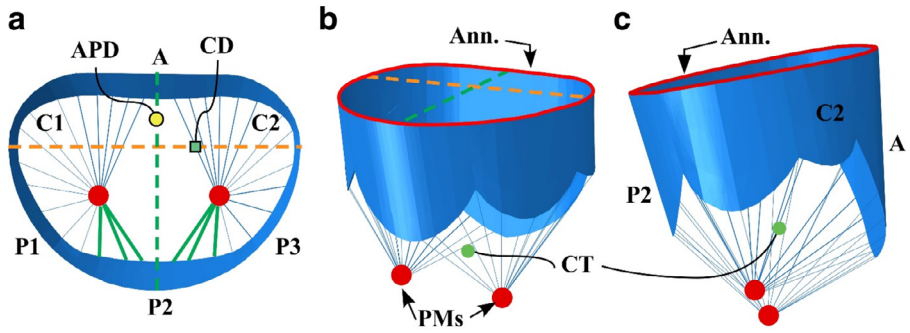

Fig. 1. MV geometry of the model at the end of diastole. (a) Atrial to ventricle view: A indicates the anterior leaflet, *C1* and *C2* the commissural leaflet scallops, *P1, P2* and *P3* the posterior leaflet scallops, and APD and CD the ateropostirial and commissures distance, respectively. (b) Perspective view: red lines indicates MV annulus. CT the chordae thendinae, and PMs the papillary muscles. (c) Lateral view. The chordae thendinae in green have been cut off to generate prolapse.

procedure also requires the investigation of the leaflet coaptation and stress pattern during the chords positioning, i.e. during the operative phase of the implant procedure. Recently, a FEM analysis was developed in order to evaluate the sutures length effect in MV repair with transapical neochord implantation [20]. However, the main focus of our present study consists in analysing the procedural and post-implant outcome of the two strategies currently in use for neochords tensioning during the repair:

- the '*all together*' strategy, i.e., all chords are tensioned contemporarily all together;
- the '*one by one*', i.e., the chords are tensioned one at the time by subsequently applying to each chord a proper tensioning with a certain order.

For both tensioning strategies, the intraoperative behavior of leaflet coaptation, the stress distribution in the valve apparatus, and the tensioning force in each chord are determined by means of numerical simulations of a generalised MV prolapse.

2. Methods

2.1. Mitral valve model

Healthy MV prevents blood backflow from the left ventricle to atrium during systole by coaptation of posterior and anterior leaflets; a number of tendinous strings (*chordae tendinae*) contribute to holding the closed valve in place, by tethering the leaflets to the ventricular wall via papillary muscles structure. Leaflets were designed to include the common anatomical segments usually identified, including the anterior leaflet scallop, *A*; the commissural leaflet scallops, *C1* and *C2*; the posterior leaflet scallops *P1, P2,* and *P3*, as represented in Fig. 1. All main parameters of valve geometry, e.g., the thickness and cross-sectional area used for the leaflets and chordae in the various portions of the model, are summarized in Table 1.

Since the proposed study is concerned essentially with the systolic phase, the dynamic motion of the annulus and papillary muscles were not simulated, keeping the annular profile fixed on a plane and maintaining a constant distance between the annulus plane and the papillary muscles (idealized as anchoring points – red dots in Fig. 1). These assumptions, which are common in the literature [21,22], are considered acceptable due to the comparative nature of this study.

Leaflets were modeled as membranes, with the isotropic hyperelastic incompressible constitutive law based on a 5th order reduced polynomial strain energy potential formulation. According to previous works concerning the analysis of MV repair [23–26],

Table 1
Dimensional parameters adopted for leaflets and chordae of the MV model. Data were set in accordance with [18,17]. APD and CD indicate the ateropostirial and commissures distance, respectively.

Leaflets				
	Anterior	*Posterior*		*Commissure*
		P2	*P1/P3*	
Height (mm)	20	13.8	11.2	8.8
Ann. Length (mm)	32.3	17.5	12.7	6.7
Area (mm^2)	457.6	204.4	123.9	51.2
Thickness (mm)	0.69	0.51		0.6
Chordae Tendineae				
Cross-sectional area (mm^2)	0.29	0.27		0.28
Annulus				
APD (mm)	22			
CD (mm)	30			
Area (mm^2)	552.7			

Table 2
Determined coefficients of Eq. (1) for anterior and posterior leaflets. (All units in MPa).

	D_1	C_{10}	C_{20}	C_{30}	C_{40}	C_{50}
Anterior leaflet	4.999	0.008	−0.073	0.742	−3.093	4.635
Posterior leaflet	6.564	0.006	0.001	0.015	−0.045	0.037

U reads:

$$U = \sum_{i=1}^{5} C_{i0}\left(\overline{I_1} - 3\right)^i + \sum_{i=1}^{5} \frac{1}{D_i}\left(J_{el} - 1\right)^{2i} \quad (1)$$

Where $\overline{I_1}$ is the first deviatoric strain invariant $\overline{I_1} = \bar{\lambda}_1^2 + \bar{\lambda}_2^2 + \bar{\lambda}_3^2$, where $\bar{\lambda}_i = J^{-\frac{1}{3}}\lambda_i$ are the deviatoric stretches, with J the total volume ratio and λ_i the principal stretches;. C_{i0} and D_i are the coefficients determined from mechanical tests performed on porcine mitral valves [27], averaging data obtained along radial and circumferential direction, and they are summarized in Table 2. The anisotropy shown by the biaxial tensile tests performed by May–Newman appears rather reduced and, given the comparative purpose of the present work, it was decided to assume an isotropic hyperelastic behavior for the leaflet's tissue.

Chords were modeled as linear elastic trusses, with Young modulus (E) equal to 40 MPa [21,28]; In the NeoChord procedure, artificial chords are usually obtained from e-PTFE *CV-4 Gore-Tex* sutures with a cross-section of 0.074 mm^2, tied to the leaflet margin with a girth hitch knot approach, resulting in two suture stands pulled in the same direction [29]. In the model, each artificial chord was represented by linear truss element with a circular cross-section of

0.148 mm^2 (i.e., equal to the sum of the cross-section of the two stands). The neochord's Young modulus was determined experimentally by performing tension testing on an e-PTFE wire. For the test, the wire was settled on the tensile testing machine (Zwick-Roll, *Zwick GmbH & Co.KG, Zwick USA*) in a wet environment of saline solution at a temperature of 37°, to recreate physiological conditions. A 40 mm initial length was used, i.e., the length of the neochords in the numerical model. Results suggested a value of the Young modulus equal to 2.3 GPa for the *CV-4 Gore-Tex suture*.

2.2. Simulations

The mitral valve was modeled by using the explicit approach with the finite element code ABAQUS (SIMULIA, Providence, RI). Leaflets and chords were represented by linear triangular membrane elements (2D elements) and truss (1D elements), respectively. The connections between the leaflets free-margin and the chordae tendineae were modeled simulating the physiological intra-leaflets insertion of the native chords as described by [30,31], on the basis of an accurate clinical analysis. In the model, along with the free-margin insertion, the native chordae elements were prolonged inside the leaflets by sharing the same nodes discretization for three nodes, thus avoiding unrealistic stress concentration and singularity points.

The nodes describing the annulus were fixed in space, allowing rotations of the leaflets elements about all axes. Similarly, the chordae were pinned at the nodes corresponding to the papillary muscles. The unloaded valve model was generated in a fully open position [32].

The closed configuration was achieved by applying a spatially uniform pressure on the ventricular side. Since the model does not describe the annulus and papillary muscles dynamics occurring during the cardiac cycle, some preliminary simulations were performed to verify the effect of the load history on the systolic configuration. In particular, the comparison between the values of the maximum principal stresses at the peak load, which were obtained applying physiologically pulsatile pressures and steady pressure conditions reached by ramping the load linearly (Fig. 2(c)), indicated lower stress in pulsatile condition, with differences inferior to 10%. Differences in term of displacement were negligible and inferior to 0.5%. Hence, the decision was taken to apply a spatially uniform pressure linearly increasing from 0 to 120 mmHg in 200 ms (corresponding to the systolic peak) to the ventricular side of the valve, for all analyzed cases. This approach significantly reduced the overall computational cost of the simulations, as well.

A reference model, including the presence and healthy function of all chordae, was run to estimate the optimal anterior–posterior leaflets coaptation achievable with the selected MV description (see Fig. 1). A MV incompetence was then simulated by detaching six central chords (see green chords in Fig. 1), leading to a central width prolapse (P2 section in Fig. 2(a)) that is the most common leaflet disease for patients who underwent NeoChord repair [33].

In the prolapsed scenario, the repair was simulated by adding four artificial neochords between the margin of the prolapsed leaflets portion and the ventricle entry site (see Fig. 2(b)), [34]. The entry site was located 40 mm apart from the annulus, according to in-vivo measurements, to form the optimal neochord trajectory implantation [35].

In the first stage of the analysis, the four sutures were not tensioned until the maximum pressure load was achieved (case of implanted but inactive artificial chords to mimic the prolapsed pre-tensioning configuration) so that the valve reached the idealized prolapse condition before the tensioning. From the end-diastole configuration, with a linear pressure load from 0 to 120 mmHg, the valve is forced to close. During this first stage of the simulation, all the artificial sutures implanted were not tensioned (i.e., one side is attached to the leaflet while the other side was free to move in order to simulate the clinical phase during which the external sutures remain outside the ventricle before the tensioning stage). In the second stage of the analysis, two different strategies for restoring the valve coaptation were pursued. In the first one, indicated as *all together* strategy (AT) the four chords were tensioned contemporarily, by applying the displacement required to restore leaflets coaptation (Fig. 3(a)). In the second strategy, indicated as *one by one* strategy (1-by-1), the four chords were tensioned one at the time by subsequently applying to each chord the same displacement as the AT case. In all simulations, for all the schemes analyzed, the tensioning was performed by imposing at the proxi-

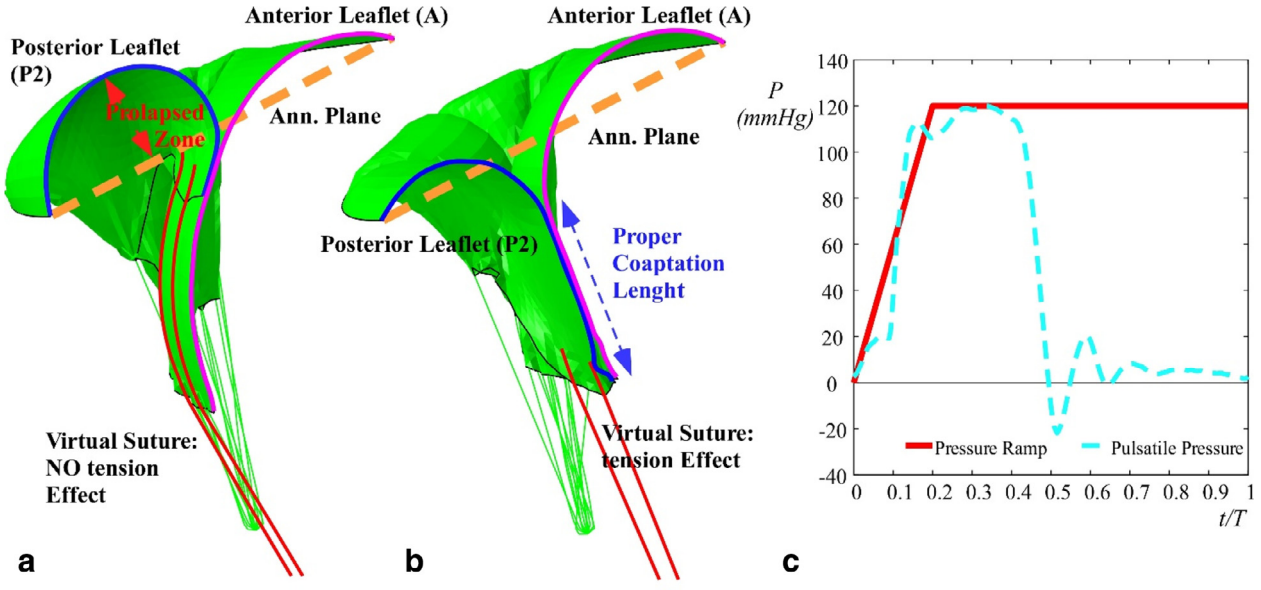

Fig. 2. Restoration of MV. (a) P2 prolapse before the tensioning of neochords (red lines). (b) P2 prolapse mitigation due to the tensioning of the neochords. Virtual sutures are inserted 3 mm far from leaflet free margin. The contact line between anterior (magenta line) and posterior (blue line) leaflet determines the coaptation length. (c) Comparison between pulsatile (dotted line) and steady pressure condition (solid line) linearly reached. The latter was applied to the ventricular surface of the valve for all simulation. (For interpretation of the references to colour in this figure, the reader is referred to the web version of this article.)

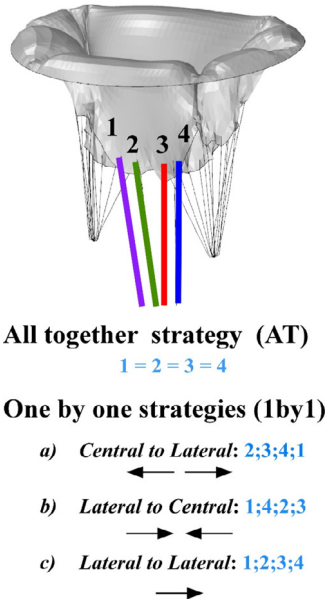

Fig. 3. Simulated protocol tensioning. In AT procedure all neochords are pulled together. In 1-by-1 procedure the chords are pulled one by one following three sequences: (a) central to lateral, (b) lateral to central, and (c) lateral to lateral. In all simulations, neochords are numbered in crescent order starting from left external position to right external position.

mal nodes of the artificial sutures the same outward displacement along the longitudinal direction. Such displacement promotes the reduction of the prolapsed portion of the posterior leaflet, since its margin moves towards the anterior one, until the repaired configuration is achieved. The prescribed displacement was set equal to 11 mm, to obtain the proper coaptation length. This value was defined after some preliminary analysis by tuning the chords displacement until the maximum coaptation length between the anterior and posterior free margin was measured at the anterior-posterior axis (see Fig. 1). In order to compare the two pulling strategies, we chose to prescribe the same displacement of the sutures in all simulations, coherently with the clinical practice, where clinicians can easily control the chordae displacement. In order to examine the different strategies commonly adopted by surgeons when repairing MV prolapse by NeoChord procedure, the following possible sequences of chord pulling were simulated (Fig. 3(b)):

(a) central to lateral pulling (1-by-1a);
(b) lateral to central (1-by-1b);
(c) lateral to lateral (1-by-1c).

3. Results

The healthy configuration of the generalized MV model produced a leaflets coaptation length along the axis of symmetry of about 8 mm, corresponding to a total contact area, $A_{c,H}$, between the anterior and posterior leaflet of about 270 mm^2. The contact area, A_c, restored during neochords tensioning procedures, normalized with $A_{c,H}$ is reported in Fig. 4.

Fig. 5 shows the contour map of the stress field computed on the treated leaflet *P2* for all analyzed configurations. A scale from 0 to 0.5 MPa was chosen to better visualize the areas of stress concentration. The maximum stress reached any point in *P2* was determined, and its evolution upon time is summarized in Fig. 6, irrespective of the position on the scallop where it was recorded.

Finally, since neochord tensioning was simulated by imposing a displacement, the corresponding force along the sutures was calculated. Fig. 7 describes the variation of the force in time for each of the four implanted neochords, for both AT (panel a) and 1-by-1 strategies (panels b-d).

4. Discussion

The MV presents a complex structure that results in a large population variability in both anatomies (e.g., the number of chordae, leaflets, and annulus shape) and size. Since, the main purpose of the study is to understand the main effects of the tensioning procedure of artificial chords during the NeoChord implantation and to generalize the results regardless the patient-specific anatomy, a model based on an idealized morphology of a population average size [21] was adopted to reproduce the MV apparatus and prolapse simulation. MV prolapse repair has the function of restoring proper leaflet coaptation. To this aim, the computed contact area at the systolic peak, A_c, normalized over the contact area estimated in healthy conditions, is chosen to provide an indication of the efficacy of the procedure. The same parameter was previously adopted in similar works [17,18], in which the dynamics of the MV is simulated through a more sophisticated patient-specific model. Results reported in Fig. 4 suggest that the restoration of MV functionality is achieved for both AT and 1-by-1 strategies.

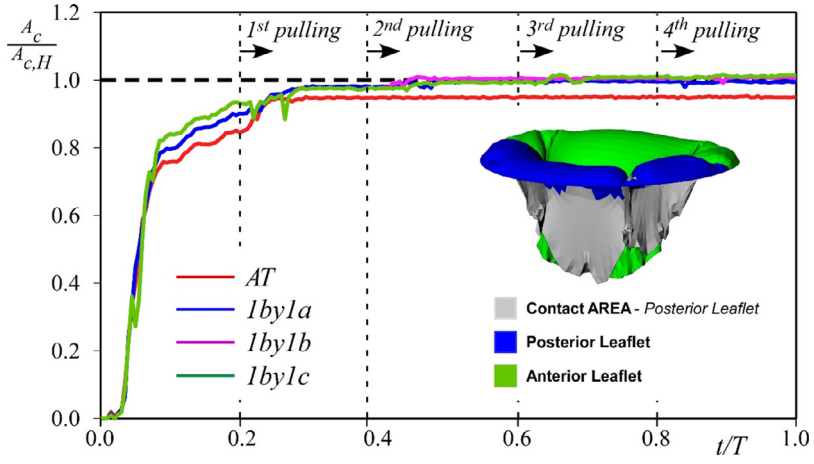

Fig. 4. Overall contact area on the Posterior leaflet during chord tensioning normalized with the contact area of the healthy configuration $A_{c,H}$. Red line represents AT strategy, blue, magenta and green lines represent 1-by-1 strategies following sequence (a), (b) and (c) of Fig. 3, respectively. (For interpretation of the references to colour in this figure, the reader is referred to the web version of this article.)

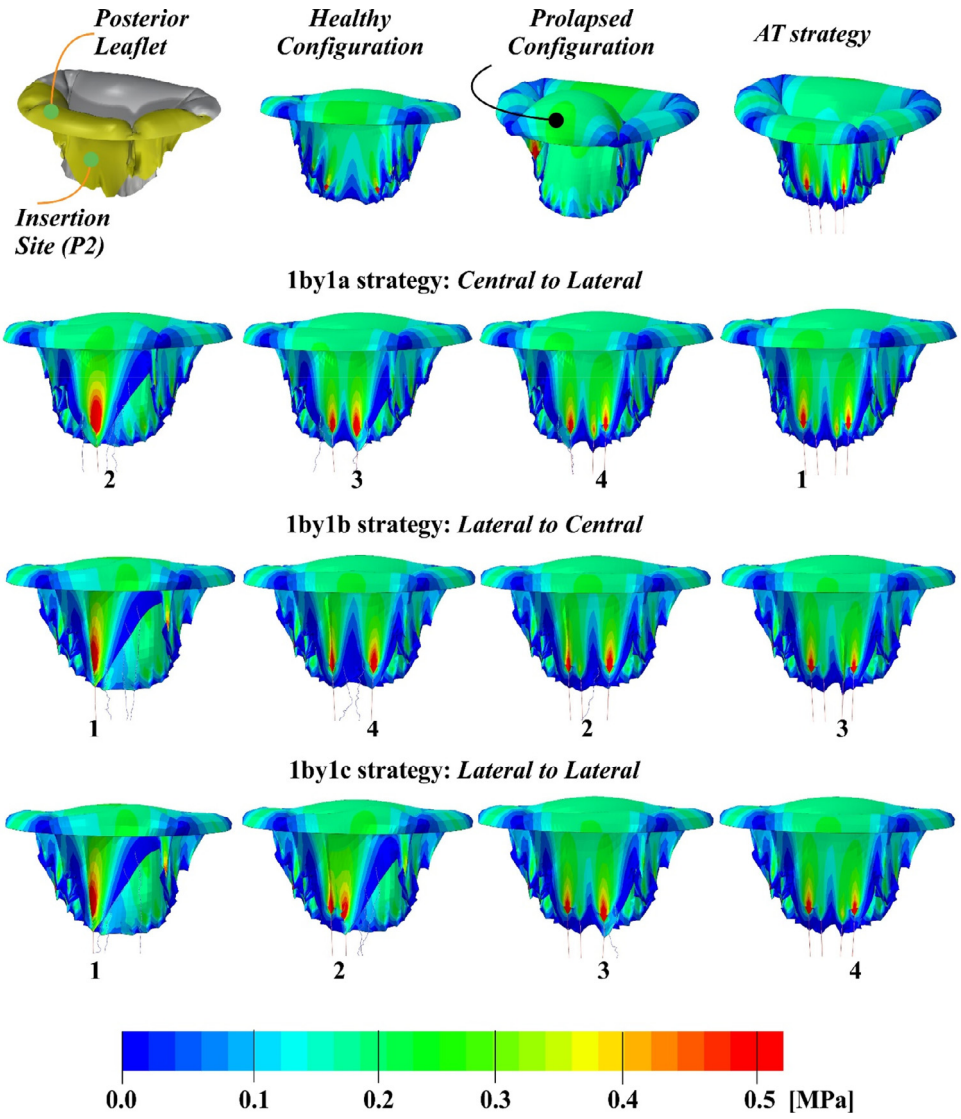

Fig. 5. MV stress patterns at systolic peak. Leaflet stress in healthy configuration, prolapsed configuration with inactive neochords, AT strategy configuration, and 1-by-1 strategy at different steps of pulling. The stress field in 1-by-1 cases is reported after the complete load of the neochord labeled by the irrespective number. (For interpretation of the references to colour in this figure, the reader is referred to the web version of this article.)

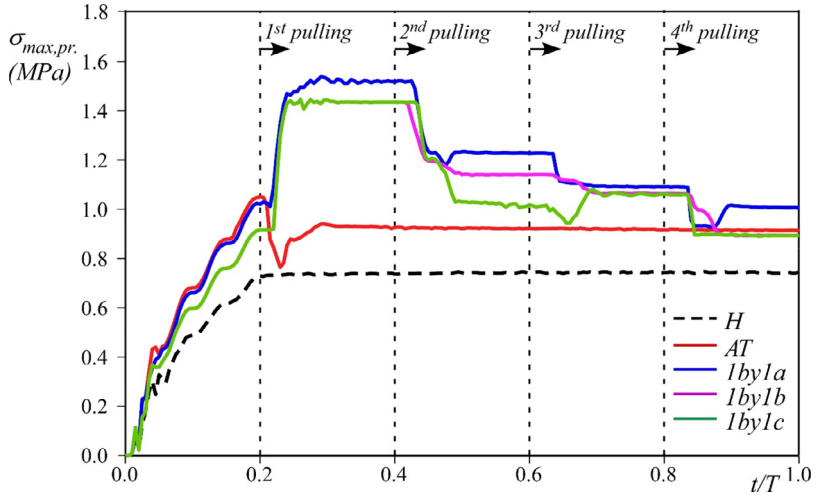

Fig. 6. Maximum principal stress calculated on the *P2* scallop during simulations. The black dotted line represents the stress calculated for the Healthy configuration (*H*). The red line represents the AT strategy. The blue, magenta and green lines represent 1-by-1 strategies following sequence (a), (b) and (c) of Fig. 3, respectively. (For interpretation of the references to colour in this figure, the reader is referred to the web version of this article.)

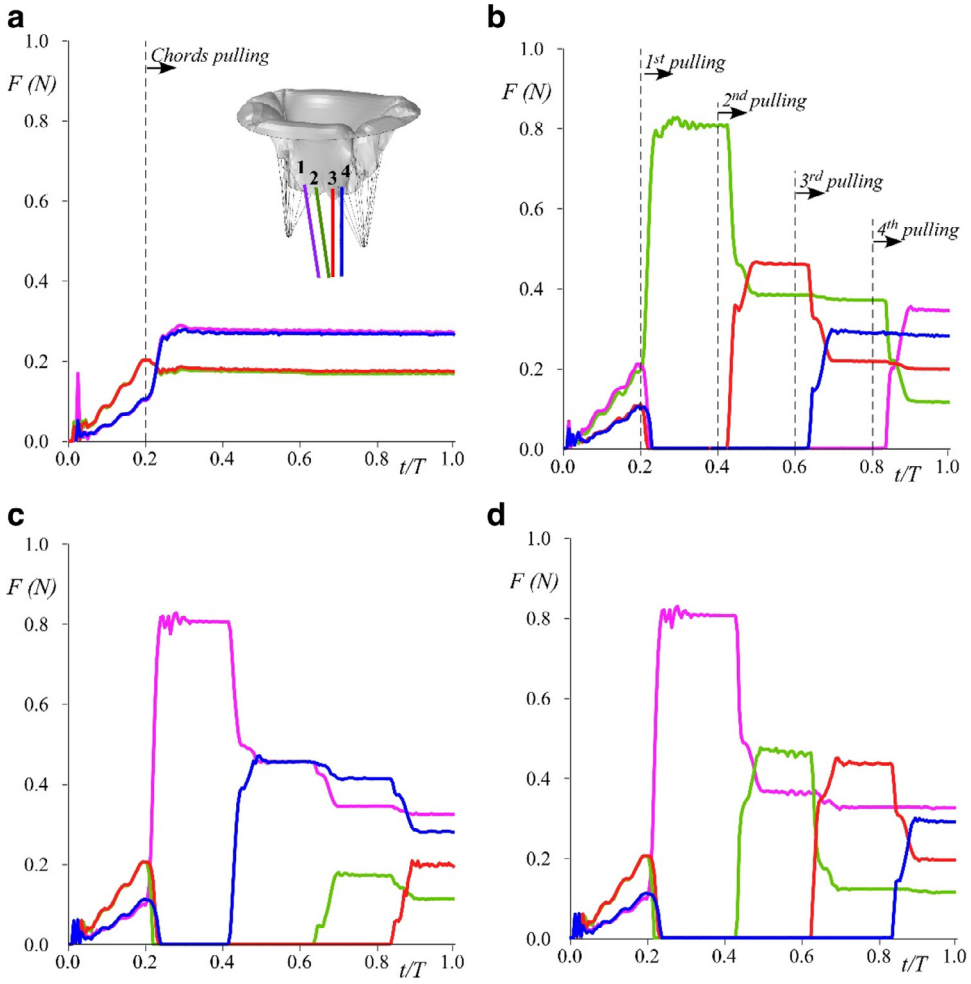

Fig. 7. Force applied by neochords during the implant in (a) AT strategy, (b) 1-by-1a (central to lateral sequence), (c) 1-by-1b (lateral to central sequence), and (d) 1-by-1c (lateral to lateral sequence).

For the AT strategy, the achieved coaptation area is about 95% of the healthy value $A_{c,H}$; whilst with the 1-by-1 strategy $A_{c,H}$ is matched or even slightly exceeded. It is also worth noting that, in the case of the 1-by-1 scheme, the first neochord tensioning already results into a coaptation area equal to the 90% of $A_{c,H}$, suggesting that MV restoration could be achieved by means of just one suture, for the present type of prolapse. However, as discussed below, the use of multiple chords allows to better diffuse stresses over a larger leaflet region, similarly to the physiological case, and distribute the load between the different chords.

The stress distribution on the valvular apparatus reported in Fig. 5 shows that, for the prolapsed configuration, portion *P2* experiences stress levels similar to the healthy case, while high-stress regions appear located at the adjacent portions of *P1* and *P3* scallops, close to the position of native chords rupture, in agreement with the literature [17]. It is worth noting that the correspondence between the present results and those obtained with a patient-specific based model confirms the reliability of the adopted simplifications. The stress pattern after the procedure is similar to the healthy case, for both *AT* and 1-by-1 tensioning. However, in 1-by-1 simulations significantly higher stress levels are obtained at different stages of the procedure. In particular, the first chord pulling causes high stress in one region around the chord insertion site. This effect is clearly mitigated after the second chord pulling, with high stress redistributed in two smaller regions; then, tensioning of the third and fourth chord reduces only slightly the amplitude of high stress regions and transfers the stress concentration in proximity to the external chords insertion. The results are partially supported by the works of Rim et al. [17], and Sturla et al. [18], which focus on the MV restoration by chords replacement considering neochordoplasty, i.e., a different surgical technique, carried out through the classical open-chest surgery. In particular, they tested a virtual repair, at peak systole, of prolapsed MV and its mitigation by implanting different numbers of chordae. The results, both in terms of stress reduction and distribution, on the posterior leaflet are consistent with the results of the present analysis. In fact, the same pattern of stress is observed at the end of the procedure, showing the maximum at the external sutures, although it results in 20% lower [17]. In Fig. 6, the analysis of the maximum stress on the valve leaflets, $\sigma_{\max}$, indicates that the 1-by-1 and AT strategies give very similar results, reaching values of about 0.9 MPa at the end of the procedure. These values are larger than the maximum stress estimated in the healthy condition, which is about 0.75 MPa. It is worth noting that the sequences of pulling in the 1-by-1 strategies can affect the stress condition on the leaflets, showing higher values when the first chord is pulled, with a $\sigma_{\max}$ of about 1.5 MPa for 1-by-1a, and 1.4 MPa with the other tensioning sequences. The tensioning of the other sutures leads to progressively lower stress levels, and at the end of the implant, we estimated additional stress of 0.9 MPa in all cases of analysis, except for the 1-by-1a strategy, which achieves $\sigma_{\max} = 1.0$ MPa (see Fig. 6).

Table 3
Forces calculated on the neochords after the implantation of the four cases analyzed. Forces are expressed in *N*.

	Neochord				Tot
	a	*b*	*c*	*d*	
AT	0.27	0.17	0.18	0.27	0.89
1-by-1a	0.34	0.10	0.20	0.28	0.92
1-by-1b	0.32	0.11	0.19	0.28	0.90
1-by-1c	0.32	0.11	0.19	0.29	0.91

The assumption of isotropic behavior, taken as an average of the radial and circumferential stress-strain curves, although may have some minor effects on the final stress distribution on the leaflets, leads to negligible differences in terms of chords tensioning forces, which are the principal aspect under investigation and essentially depend on the transvalvular pressure and on the shape of the leaflets.

The stress distribution on the leaflets is related to the tensile force measured in the sutures (Fig. 7). Neochords pulled according to the AT procedure are subjected to a symmetrical force distribution, with a difference of about 30% between the force acting on the central and lateral insertions (0.18 N and 0.27 N, respectively, see Fig. 7(a)). 1-by-1 simulations show that the tensioning order affects the measured force. Specifically, tensioning a chord reduces the force applied to the chords previously pulled, and the reduction strongly depends upon the maneuver order and chords position. For instance, in the 1-by-1a case (Fig. 7(b)) the force on the neochord pulled first (neochord 2) diminishes as soon as neochord 3 is pulled (F reduction around 50%) with a further reduction, when neochord 1 is pulled (F reduction around 40%); i.e., the force on a chord reduces as soon as nearby chords become active. Results also show that no symmetry can be recognized in the final force distribution with respect to either neochord position or tensioning order. Moreover, the force is found to vary in the range 0.3–0.35 N for the external chords and in the range 0.1–0.2 N for the central one, showing that the maximum force difference between lateral and central artificial elements can be as large as 80%. The latter finding suggests that a central neochord can possibly result approximately unloaded at the end of neochords implantation, as reported by surgical clinical practice.

In all cases, the force on one neochord is well below the failure force of the suture, which is about 16 N, according to the GORE-TEX® SUTURE ePTFE manual. Finally, values of end procedure force applied to each neochord (see Table 3) also show that the overall force on the group does not significantly vary between the four simulated strategies of pulling, further reinforcing the idea that differences in force repartition is due to the pulling sequence. In summary, the AT procedure guarantees an almost symmetric distribution of the tensioning force on the neochords and the minimum stress level during the implant procedure, but does not fully restore the healthy contact area. One-by-one strategies allow optimizing the coaptation area, although the stresses generated in the leaflets following the procedure were equal to that in the AT procedure, except for the central to lateral tensioning sequence, which presents a higher stress level and it is proved to be the least appropriate. Furthermore, the 1-by-1 strategies may lead to almost inactive chords if care is not given to this aspect.

5. Study limitations

The present study is limited to the *P2* central prolapse, i.e. the most common MV prolapse. A different stress force distribution may be expected for the lateral (*P1–P2* or *P2–P3*) and the anterior (*A*) prolapse. In particular, in the former, due to its asymmetry, the tensioning of the suture is more likely to depend on the pulling strategy.

The use of membrane elements instead of shell elements, neglecting the response to bending, leads to some minor change in the contact area which, due to the higher flexibility of the selected element, can result a bit overestimated. Consequently, stresses on the leaflets can result slightly lower (up to 10%), whereas the force exerted by the sutures does not experience any significant change.

The use of both more realistic geometric configuration and more physiologic boundary condition can further improve the results and highlight additional aspects of the NeoChord implant. It can be foreseen that, lastly, application of the presented approach to patient-specific anatomies may provide a useful tool for procedural planning, improving the efficacy of the treatment.

6. Conclusions

The present investigation compares the two most common tensioning procedures adopted in the transapical neochords implantation for mitral valve prolapse repair, i.e., ‘all together’ and ‘one by one’ pulling approach. The study was performed on a generalized MV morphology, with prolapsed P2 scallop. Although idealized geometries and simplified constitutive behaviors were assumed, the study captures some of the clinical effects observed by surgeons, e.g., the unloading of previously pulled neochords.

The close similarity between healthy and repaired configuration obtained for all investigated strategies confirms the reliability and efficacy of the preferred surgical choice of four chords to treat the prolapse here considered.

Differences found in the results concerning coaptation area, stress distribution, and force on the neochords for AT and 1-by-1 repair suggest that the 1-by-1 lateral to central and lateral to lateral approaches are the most suitable solutions to reach maximum coaptation and maintaining operative leaflets stresses closer to those experienced in healthy conditions. AT strategy appears more conservative in terms of maximum stress during the intra-operative insertions since all the chords are activated at the same time, though this happens at the expense of the optimal valve closure.

Though this first study was based on a generalized symmetrical model, the robustness and reduced computational cost of the presented methodological approach makes it is suitable to be adopted for the clinical planning of the treatment in patient-specific cases. In addition, this model can represent the first step towards a more sophisticated platform, using patient-specific images to optimize the surgeical procedure.

Ethical approval

Not required.

Declaration of Competing Interest

None of the authors has any relationship with industry or financial associations that might pose a conflict of interest in connection with this work.

Acknowledgments

Authors thank Fondazione Cariparo, Padova, Italy, for funding Ph.D. fellowship of Luigi Di Micco. The Fondazione Cariparo had no involvement in the study design, in the collection, analysis, and interpretation of data, in the writing of the manuscript, and in the decision to submit the manuscript for publication.

This research has been also partially supported by the Fondazione Ing. Aldo Gini, Padova, Italy.

References

[1] Biglino G, Capelli C, Bruse J, Bosi GM, Taylor AM, Schievano S. Computational modelling for congenital heart disease: how far are we from clinical translation? Heart 2017;103(2):98–103.
[2] Toninato R, Salmon J, Susin FM, Ducci A, Burriesci G. Physiological vortices in the sinuses of Valsalva: an in vitro approach for bio-prosthetic valves. J Biomech 2016;49(13):2635–43.
[3] Burriesci G, Peruzzo P, Susin FM, Tarantini G, Colli A. In vitro hemodynamic testing of Amplatzer plugs for paravalvular leak occlusion after transcatheter aortic valve implantation. Int J Cardiol 2016;203:1093–9.
[4] Votta E, et al. Toward patient-specific simulations of cardiac valves: state-of-the-art and future directions. J Biomech 2013;46(2):217–28.
[5] Susin FM, Tarzia V, Bottio T, Pengo V, Bagno A, Gerosa G. In-vitro detection of thrombotic formation on bileaflet mechanical heart valves. J Heart Valve Dis 2011;20(4):378–86.
[6] Choi A, Mcpherson DD, Kim H. Computational virtual evaluation of the effect of annuloplasty ring shape. Int J Numer Method Biomed Eng 2016;02831(September):1–11.
[7] Members AF, et al. Guidelines on the management of Valvular heart disease (version 2012) the joint task force on the management of valvular heart disease of the European society of cardiology (ESC) and the European association for cardio-thoracic surgery (EACTS). Eur Heart J 2012;33(19):2451–2496.
[8] Nishimura RA, Otto CM, Bonow RO, Carabello BA, Erwin JP 3rd, Guyton RA, et al. 2014 AHA/ACC guideline for the management of patients with valvular heart disease: A report of the American College of Cardiology/American Heart Association Task Force on Practice Guidelines. Circulation 2014;129(23):e521–643.
[9] Castillo JG, Solís J, González-Pinto Á, Adams DH. Surgical echocardiography of the mitral valve. Rev Española Cardiol (Engl Ed) 2011;64(12):1169–81.
[10] Colli A, Bizzotto E, Pittarello D, Gerosa G. Beating heart mitral valve repair with neochordae implantation: real-time monitoring of haemodynamic recovery. Eur J Cardio-thoracic Surg 2017;52(5):991–2.
[11] Colli A, Bellu R, Pittarello D, Gerosa G. Transapical off-pump neochord implantation on bileaflet prolapse to treat severe mitral regurgitation. Interact Cardiovasc Thorac Surg 2015:ivv192.
[12] Colli A, et al. Acute safety and efficacy of the neochord procedure. Interact Cardiovasc Thorac Surg 2015;20(5):575–81.
[13] Bajona P, Zehr KJ, Liao J, Speziali G. Tension measurement of artificial chordae tendinae implanted between the anterior mitral valve leaflet and the left ventricular apex: an in vitro study. Innovations (Phila) 2008;3(1):33–7.
[14] Bajona P, Katz WE, Daly RC, Zehr KJ, Speziali G. Beating-heart, off-pump mitral valve repair by implantation of artificial chordae tendineae: an acute in vivo animal study. J Thorac Cardiovasc Surg 2009;137(1):188–93.
[15] Jensen H, et al. Transapical neochord implantation: is tension of artificial chordae tendineae dependent on the insertion site? J Thorac Cardiovasc Surg 2014;148(1):138–43.
[16] Reimink MS, Kunzelman KS, Verrier ED, Cochran RP. The effect of anterior chordal replacement on mitral valve function and stresses: a finite element study. Asaio J 1995;41(3):M754–62.
[17] Rim Y, Laing ST, McPherson DD, Kim H. Mitral valve repair using ePTFE sutures for ruptured mitral chordae tendineae : a computational simulation study. Ann Biomed Eng 2014;42(1):139–48.
[18] Sturla F, et al. Biomechanical drawbacks of different techniques of mitral neochordal implantation: when an apparently optimal repair can fail. J Thorac Cardiovasc Surg 2015;150(5):1303–12.
[19] Morgan AE, Pantoja JL, Grossi EA, Ge L, Weinsaft JW, Ratcliffe MB. Neochord placement versus triangular resection in mitral valve repair: a finite element model. J Surg Res 2016;206(1):98–105.
[20] Gaidulis G, Votta E, Selmi M, Aidietien S. Numerical simulation of transapical off-pump mitral valve repair with neochordae implantation. Technol Heal Care 2018;26.
[21] Lau KD, Diaz V, Scambler P, Burriesci G. Medical engineering & physics mitral valve dynamics in structural and fluid–structure interaction models. Med Eng Phys 2010;32(9):1057–64.
[22] Kunzelman KS, Einstein DR, Cochran RP. Fluid-structure interaction models of the mitral valve: function in normal and pathological states. Philos Trans R Soc B Biol Sci 2007;362(1484):1393–406.
[23] Avanzini A, Donzella G, Libretti L. Functional and structural effects of percutaneous edge-to-edge double-orifice repair under cardiac cycle in comparison with suture repair. Proc Inst Mech Eng H: J Eng Med 2011;225(10):959–71.
[24] Avanzini A. A computational procedure for prediction of structural effects of edge-to-edge repair on mitral valve. J Biomech Eng 2008;130(3):031015.
[25] Dal Pan F, Donzella G, Fucci C, Schreiber M. Structural effects of an innovative surgical technique to repair heart valve defects. J Biomech 2005;38(12):2460–71.
[26] Prescott B, Abunassar CJ, Baxevanakis KP, Zhao L. Computational evaluation of mitral valve repair with Mitraclip. Vessel Plus 2019;2019:0–10.
[27] May-Newman K, Yin FC. Biaxial mechanical behavior of excised porcine mitral valve leaflets. Am J Physiol Circ Physiol 1995;269(4):H1319–27.
[28] Kunzelman K, Reimink MS, Verrier ED, Cochran RP, Frater RWM. Replacement of mitral valve posterior chordae tendineae with expanded polytetrafluoroethylene suture: a finite element study. J Card Surg 1996;11(2):136–45.
[29] Colli A, et al. Transapical off-pump mitral valve repair with neochord implantation (TOP-MINI): step-by-step guide. Ann Cardiothorac Surg 2015;4(3):295.
[30] Muresian H. The clinical anatomy of the mitral valve. Clin Anat 2009;22(1):85–98.
[31] Rim Y, et al. Uncertainty quantification of inflow boundary condition and proximal arterial stiffness coupled effect on pulse wave propagation in a vascular network. Ann Biomed Eng 2016;9(1):85–98.
[32] Votta E, Caiani E, Veronesi F, Soncini M, Montevecchi FM, Redaelli A. Mitral valve finite-element modelling from ultrasound data: a pilot study for a new approach to understand mitral function and clinical scenarios. Philos Trans R Soc A Math Phys Eng Sci 2008;366(1879):3411–34.
[33] Colli A, et al. Prognostic impact of leaflet-to-annulus index in patients treated with transapical off-pump echo-guided mitral valve repair with neochord implantation. Int J Cardiol 2018;257:235–7.
[34] Colli A, et al. Transapical off-pump mitral valve repair with neochord implantation: early clinical results. Int J Cardiol 2016;204:23–8.
[35] Colli A, et al. CT for the transapical off-pump mitral valve repair with neochord implantation procedure. JACC Cardiovasc Imaging 2017;10(11):1397–400.